Development of Low- and High-Birefringence Optical Fibers

DAVID N. PAYNE, ARTHUR J. BARLOW, AND JENS J. RAMSKOV HANSEN, MEMBER, IEEE

(*Invited Paper*)

Abstract—**The polarization properties of single-mode optical fibers are easily modified by environmental factors. While this can be exploited in a number of fiber sensor devices, it can be troublesome in applications where a stable output polarization-state is required. Fibers with both low and high birefringence have been developed to enhance or diminish their environmental sensitivity, and recent progress in each area is reviewed. Low-birefringence fibers are described which are made by spinning the preform during the draw. In addition, developments in high-birefringence fibers which maintain a polarization state over long lengths are summarized. The effect on performance of external factors such as bends, transverse pressure, and twists is analyzed. Consideration is also given to polarization mode-dispersion as a potential limiting factor in ultrahigh bandwidth systems.**

I. Introduction

SINGLE-MODE optical fibers are birefringent as a result of an (often unintentional) lack of circular symmetry in the core cross section. This and an associated stress anisotropy allows the fiber to support two nearly degenerate orthogonally polarized modes with a small phase-velocity difference. When only one of the modes is excited, the state of polarization remains constant along the length of the fiber, whereas if both are present, the polarization state evolves cyclically as the modes beat together in phase relationship. In a typical fiber the magnitude of this intrinsic birefringence is relatively small and it is found that it can be severely modified by environmental factors such as pressure, twists, and bends which, in a practical installation, vary in an unpredictable manner. The overall fiber birefringence, and thus the output polarization state cannot be predetermined and, moreover, vary with time and temperature.

The unpredictability of the polarization state presents a problem in fiber interferometers where colinearity of the interfering beams is required [1]-[4], in coupling to polarization-sensitive integrated optics [5] and in phase-coherent detection schemes for communications [6]. A well-established solution is the "polarization-maintaining" fiber [7] in which the internal birefringence is increased to a level well above that likely to be caused by environmental effects. The waveguide then appears essentially length-invariant, since external perturbations are swamped by the high level of internal birefringence. Thus, a single linearly polarized mode can be selected and sustained without coupling energy to its orthogonally polarized partner.

Manuscript received November 12, 1981.

D. N. Payne and A. J. Barlow are with the Department of Electronics, University of Southampton, Southampton, England.

J. J. Ramskov Hansen was with the Department of Electronics, University of Southampton, Southampton, England. He is now with NKT, Copenhagen, Denmark.

By contrast, in a polarimetric sensor the variation in the output polarization state is exploited as a measure of the magnitude of an external effect. Thus, in the Faraday-effect current monitor [8], [9], the magnetic field surrounding a conductor causes a rotation of the plane of polarization in the fiber, while in an acoustic or magnetic-field sensor, vibration or magnetostriction of a former upon which the fiber is wound applies pressure and induces linear birefringence [10]. In these cases the internal fiber-birefringence can interfere with the induced birefringence to reduce the sensitivity [8], [11], [12], and a low-birefringence fiber is an advantage.

Several in-line fiber devices have been constructed [13]-[15] which utilize the birefringence induced by controlled bends and twists to provide the fiber analog of discrete birefringent spectral-filters and compensators. Internal fiber birefringence unpredictably modifies the required birefringence and, since it is temperature sensitive, detracts from device stability. Again, a low-birefringence fiber is required.

Birefringence also leads to a group-delay difference between orthogonally polarized modes which may significantly reduce the telecommunication bandwidth [16]. One solution is to select only one mode and prevent energy transfer to the other by using a high-birefringence polarization-maintaining fiber. However, in the event of some power transfer occurring, the pulse dispersion will be large. The alternative solution is to use a low-birefringence fiber in which the group-velocity difference is negligible. However this approach does not provide a defined output polarization-state.

There is clearly a need for low and high-birefringence fibers in sensor and communications technology and it is our purpose to review progress in the development of both. We will be concerned with more recent advances, since two comprehensive reviews [17], [18] have adequately covered earlier work. Emphasis is placed on low-birefringence fibers, low-loss high-birefringence fibers and polarization mode-dispersion. In addition, an analysis is described which allows a comparison to be made of the effects of twists and bends on various polarization-maintaining fibers, which also has relevance to polarimetric sensors. We start with a review of fiber polarization properties and their response to external factors.

II. Birefringence in Single-Mode Fibers

A. Linear Birefringence

"Single-mode" fibers with an asymmetric cross section propagate two orthogonal linearly polarized modes with axes aligned with those of fiber symmetry. These modes propagate unchanged in the absence of length-dependent variations in the fiber, with a difference $\delta\beta$ (the birefringence) in their propaga-

0018-9480/82/0400-0323$00.75

tion constants. The fiber polarization properties can then be modeled [19] as a discrete linearly birefringent element whose retardance $R(z)$ is proportional to fiber length z

$$R(z) = \delta\beta z. \tag{1}$$

Two commonly used parameters which are useful in describing fibers with length-invariant properties are the normalized linear-birefringence B and the mode beat-length L_p at which the polarization state is periodically repeated

$$B = \frac{\lambda}{2\pi}\delta\beta = \frac{\lambda}{2\pi}\frac{R(z)}{z} = \delta n \tag{2}$$

$$L_p = \frac{2\pi}{\delta\beta} = \frac{\lambda}{B} \tag{3}$$

where λ is the free-space wavelength of light and δn the difference in mode effective-indexes. In general, B comprises both stress anisotropy B_s and a waveguide shape component B_G.

Whereas for a low-birefringence fiber an increase in L_p is desired, in a polarization-maintaining fiber we wish to decrease the value of L_p (i.e., increase the birefringence) in order to reduce the likelihood of power transfer from the required to the unwanted mode. It is well known from coupled-mode theory that maximum power transfer between modes occurs when the period of external perturbations matches that of the beat-length [20]. The natural stiffness of the fiber resists perturbations with periods less than about 1 mm and consequently, this sets a target for L_p. We will show, however, using uniform mode-coupling, that power transfer to the unwanted mode also occurs for perturbation periods which are multiples of L_p (Section V).

B. Circular Birefringence

Although it is possible to conceive externally applied stress whose direction varies azimuthally along the fiber length, the most common cause of circular birefringence is fiber twist [21], [22]. Twist introduces a torsional stress, which by the photoelastic effect, leads to an optical-activity in proportion to the twist. For a uniform twist rate ξ and in the absence of linear birefringence, the fiber can be modeled as a discrete polarization rotation element with rotation $\Omega(z)$ which increases linearly with fiber length

$$\Omega(z) = g'\xi z = \alpha z \tag{4}$$

where $g' = 0.073$ for silica [22], [23] and α is the optical rotation/unit length. The two normal modes are now left and right circularly polarized with difference in propagation constants $\delta\beta_{\text{circ}} = 2g'\xi$.

C. Linear and Circular Birefringence

If constant linear and circular birefringence are simultaneously present (e.g., in a uniformly twisted elliptical-core fiber), the two fiber modes are elliptically polarized in a coordinate system which rotates with the twist [22], [24]. In a *fixed* coordinate system it is possible to represent the fiber polarization properties as a combination of a discrete rotator and retarder element [23], [24]. However, the values of these two elements are now interdependent and are not simply additive; moreover, they vary cyclically as we progress down the fiber length. In this case a Poincaré sphere representation of the polarization evolution with length is helpful [22], although in order to specify the fiber primary properties we shall use B and its circular equivalent $B_{\text{circ}} = \lambda g'\xi/\pi$.

D. Sources of Mode Coupling

Energy transfer between modes in a birefringent fiber is caused primarily by external perturbations which introduce a birefringence whose axes do not coincide with those of the fiber. Thus, index profile, numerical aperture, and diameter variations do not cause significant mode-coupling, provided the fiber axes of symmetry remain unchanged. On the other hand, bends, transverse pressure, and twists introduce linear and circular birefringence.

1) Bends: Bending a fiber results in a stress-induced linear-birefringence with a fast axis in the plane of the bend [14], [25]. For silica $\delta\beta_B$ is given by

$$\delta\beta_B = \pi\frac{EC}{\lambda}\left(\frac{r}{R}\right)^2 \simeq -\frac{0.85}{\lambda}\left(\frac{r}{R}\right)^2 \text{ rads/m} \tag{5}$$

where $E = 7.75 \times 10^9$ kg/m^2 is Young's modulus, $C(0.633\ \mu\text{m}) \simeq -3.5 \times 10^{-11}$ m^2/kg is the stress-optical coefficient, and r and R are the radii of the fiber and bend, respectively. C varies slightly with wavelength. A bend causes maximum disturbance to the fiber birefringence, and thus, greatest mode-coupling, when the plane of the bend is at 45° to the fiber birefringent axes.

2) Pressure: Transversely applied pressure similarly induces a linear-birefringence $\delta\beta_p$ with fast axis in the direction of applied compression [26], [27]. For silica

$$\delta\beta_p = 8\frac{C}{\lambda}\left(\frac{f}{r}\right) \simeq \frac{-2.8 \times 10^{-10}}{\lambda}\left(\frac{f}{r}\right) \text{ rads/m} \tag{6}$$

where f is the applied force/unit fiber length in kg/m. Again pressure is most effective when applied at 45° to the fiber birefringent axes.

3) Twists: Twist introduces a polarization rotation as given in (4) above. In a linearly birefringent fiber, an apparent optical rotation component also exists which is unrelated to the photoelastic effect, and is due to the precession of the fiber birefringent axes. Small twists of the fiber axes of symmetry commonly occur during the drawing process and as a result, the fiber exhibits an apparent permanent optical-activity [19], [28].

4) Magnetic Fields: When a longitudinal magnetic field H is applied to the fiber, the Faraday effect rotates the plane of polarization through an angle α_F/unit length given by

$$\alpha_F = V_0 H \text{ rads/m} \tag{7}$$

where $V_0 \simeq 4.5 \times 10^{-6}$ rads/A is the Verdet constant for silica [8]. For unidirectional propagation, Faraday rotation produces an effect similar to that caused by torsion.

5) Temperature: Differential thermal-expansion between a fiber and its support structure (for example, a spool), results in

transverse forces and is often the main cause of time variation in the output polarization-state. In addition, the fiber internal birefringence is temperature sensitive [29] owing to 1) the temperature dependence of the stress-optic coefficient and 2) the differential thermal-expansion between core and cladding. Results obtained in our laboratory on strain-induced high-birefringence fibers [the fiber of Fig. 2(b)] gave a variation of B of $\simeq 0.1$ percent/°C. Changes in internal fiber birefringence due to temperature do not cause mode coupling, since the axes of fiber symmetry remain unchanged; nevertheless, if both modes carry power, their phase-relationship, and hence the output polarization-state can vary considerably.

The interaction of the above external effects with the internal fiber birefringence and the consequences for polarization-maintaining fibers will be treated in a subsequent section.

E. Random Mode-Coupling

In the presence of random combinations of twists, bends, and applied pressure, the fiber can still be modeled as a combination of a discrete retarder and rotator, but with values having little relation to an intrinsic fiber property, since they depend on the external perturbations and vary randomly for different fiber lengths. Note, however, that it is always possible to find principal axes for which linearly polarized light will emerge linearly polarized (although usually rotated) from the fiber, and eigenstates of polarization which traverse the fiber unchanged [22]. These too will differ for each fiber length and are also likely to drift with time as the external perturbations change.

III. Low-Birefringence Fibers

A. Conventional Approach

Early attempts at making low-birefringence fibers [30], [31] were aimed at reducing 1) the waveguide shape birefringence B_G by maintaining a highly circular core and 2) the elastooptic anisotropy B_S by decreasing the residual core stress. These objectives were achieved by careful attention to fabrication techniques.

The calculated contribution B_G due to core ellipticity alone is plotted in Fig. 1 for operation at the higher mode cutoff (normalized frequency $V = 2.4$ for near-circular step-index fibers). It can be seen for values of $(a/b - 1) < 0.2$ (a and b are the core semimajor and semiminor axes), the curve is linear [32], since B_G is proportional to $(\Delta n)^2 \cdot (a/b - 1)$. Here Δn is the index-difference between core and cladding. Thus by keeping Δn low and attaining a circularity better than 0.1 percent it was possible to manufacture a fiber (*GSB*2 in Fig. 1) with a beat length $L_p = 140$ m at $\lambda = 0.633$ μm [31]. The cross section of this fiber is shown in Fig. 2(a).

Experience with a number of similar fibers gave low but variable birefringence results, as illustrated in the upper section of Fig. 3, and this was attributed to the inability to control the internal stress anisotropy B_S. The residual stress results from differential thermal contraction between core, cladding, and substrate materials on cooling to room temperature, and can be relatively large. Thus, a small asymmetry in the fiber cross

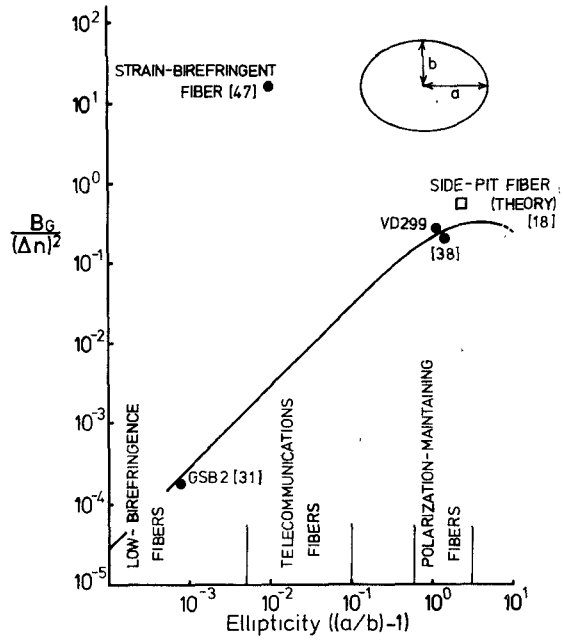

Fig. 1. Normalized fiber shape-birefringence plotted as a function of core ellipticity ($a/b - 1$), assuming operation at the higher mode cutoff. Dots give experimental results for low- and high-birefringence fibers with appropriate reference. VD299 is a shape and stress-birefringent fiber whose cross section is shown in Fig. 2(b). For comparison, a stress-birefringent fiber [47] is marked, with cross section given in Fig. 2(c). Also marked (open square) is the theoretical prediction [18] for side-pit fibers having $(a/b - 1) = 2.33$.

section produces a large stress imbalance and leads to substantial anisotropy in the core material. This conclusion was emphasized by fibers which exhibited considerably lower birefringence than allowed by their waveguide component B_G, calculated from the measured core ellipticity. Normally, B_G and B_S act in unison, provided the expansion coefficient of the core exceeds that of the cladding. If in the three-layer structure used for these fibers the core expansion-coefficient is substantially less than that of the B_2O_3-doped cladding, it is possible for B_S to oppose B_G. Evidence that this occurred in some fibers was provided by gently heating the fibers to reduce the internal stress, when it was observed that the birefringence *increased*. This leads us to speculate that a fiber could be designed with $B_S - B_G = 0$, which would be insensitive to a production spread in ellipticity, since both B_S and B_G are approximately proportional to ellipticity.

B. Spun Fibers

When a linearly birefringent fiber is twisted [21], [22], at a rate ξ rads/m, the azimuth of the fiber elliptic cross section and hence the local principal-axes precess. The fiber can be considered as composed of individual local sections having a length of a quarter twist-period and linear-birefringence which alternates in sign. Thus, although each local section may have a relatively high linear-birefringence, its effect is compensated by the next rotated section. The outcome is to produce a net retardance $R(z)$ which oscillates between a small positive and negative value along the fiber length. Thus, twist can be used

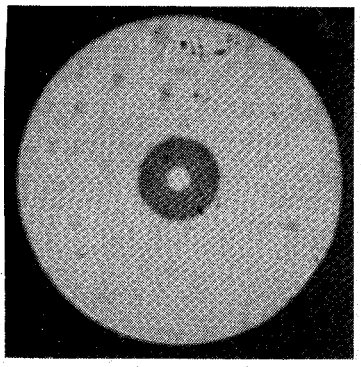

(a)

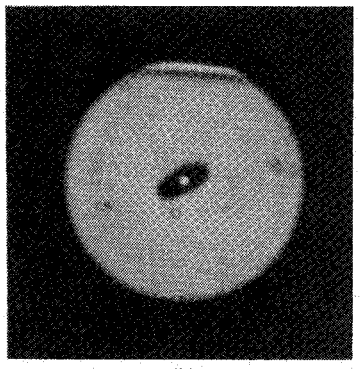

(b)

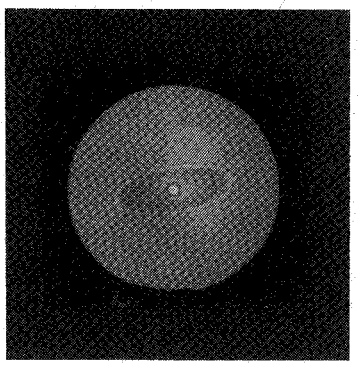

(c)

Fig. 2. Cross sections of low and high-birefringence fibers. (a) Low-birefringence fiber GSB2 [31] has a GeO_2/SiO_2 core, B_2O_3/SiO_2 cladding, and silica substrate. (b) High-birefringence fiber VD299 has stress and shape birefringence, giving $L_p(0.633\ \mu m) = 2$ mm. Core is GeO_2/SiO_2 with $a/b = 2.2$, $\Delta n = 0.035$, cladding is B_2O_3/SiO_2, substrate is silica. (c) High-birefringence fiber with large stress-anisotropy and circular core [47]. Core is GeO_2/SiO_2, cladding is $GeO_2/B_2O_3/SiO_2$ within silica substrate. Core is optically buffered from cladding by a thin silica layer to give low loss.

to reduce the fiber linear birefringence [33], although it simultaneously introduces an elastooptic rotation α as in (4). The interaction between the local linear and circular birefringence leads to net values of the retardance $R(z)$ and rotation $\Omega(z)$ given by [23]

$$R(z) = 2\sin^{-1}\left[\frac{1}{(1+q^2)^{1/2}}\sin\gamma z\right] \tag{8}$$

$$\Omega(z) = \xi z + \tan^{-1}\left[-\frac{q}{(1+q^2)^{1/2}}\tan\gamma z\right] \tag{9}$$

where

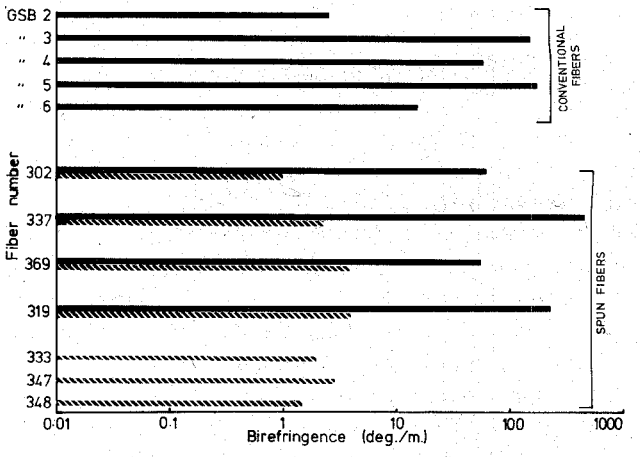

Fig. 3. Results obtained for a series of low-birefringence fibers. Upper section is for conventional low-birefringence fibers of the type illustrated in Fig. 2(a). The lower section is for fibers of a similar design and demonstrates the large improvements obtained by preform spinning. In some cases results are given for unspun (solid bars) and spun (hatched bars) sections of the same fiber.

$$q = \frac{2(\xi - \alpha)}{\delta\beta} \tag{10}$$

$$\gamma = \tfrac{1}{2}(\delta\beta^2 + 4(\xi - \alpha)^2)^{1/2}. \tag{11}$$

Here $\delta\beta$ is the linear birefringence of the untwisted fiber and comprises both shape and stress anisotropy.

If instead of twisting the fiber, we spin the preform during drawing [23], [34], [35], no circular birefringence will be present ($\alpha = 0$) because the fiber is in a viscous state at the high fiber-forming temperature and cannot support significant shear stress. If the spin rate $\xi \gg \delta\beta$ then the magnitude of the retardance oscillations become negligibly small, i.e.,

$$R(z) = \frac{\delta\beta}{\xi}\sin\xi z \tag{12}$$

and the rotation $\Omega(z) \to 0$. The internal shape and stress birefringences B_G and B_S are reduced by the ratio of the spin pitch $P = 2\pi/\xi$ to the unspun mode beat-length $L_p = 2\pi/\delta\beta$. For small ratios the fiber appears virtually isotropic. Thus, provided $P \ll L_p$, any fiber, even a high-birefringence fiber, can be transformed into a low-birefringence fiber by preform spinning. This was demonstrated by spinning a fiber having a highly elliptical cladding ($a/b - 1 \simeq 1.5$), circular substrate, and L_p ($0.633\ \mu m$) = 19 mm. The spiraling cladding with a spin pitch $P = 1.2$ mm can be clearly seen in Fig. 4. The resulting fiber had $P/L_p = 0.06$ and, as predicted by (12), exhibited a negligibly small linear and circular birefringence.

Further measurements which compare the birefringence in unspun and spun sections of fiber from a number of preforms are given in Fig. 3 and illustrate the large reductions routinely obtainable. At least an order of magnitude improvement is normally observed, bringing the residual birefringence close to the limits of measurement (~1°/m). Residual optical rotation is also found to be <1°/m.

It might be thought that the high-temperature spinning process helps to circularize the fiber geometry and so reduces the birefringence. However, the fiber still possesses a similar *local* birefringence to that in the unspun fiber, as can be demonstrated

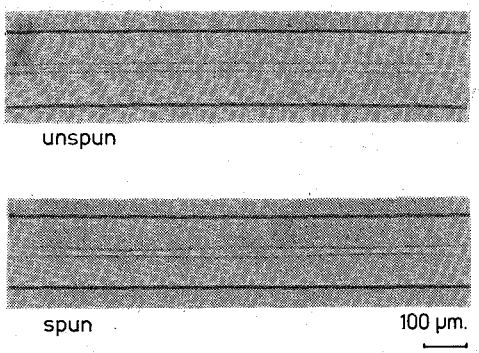

Fig. 4. Transverse view of high-birefringence fiber with elliptical cladding (upper) and after spinning (lower).

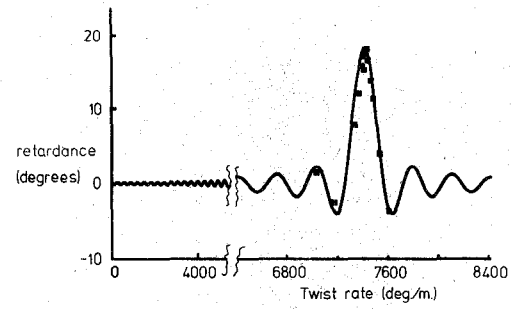

Fig. 5. Retardance in a fiber spun at a nominal $P = 5$ cm when untwisted after drawing. Solid line is the theoretical prediction according to (8) and is fitted to the data. Points are experimental values. Note the abscissa has a scale change.

by twisting the fiber in a direction to unwind the frozen-in twist. The linear birefringence should reappear, together with an optical rotation due to the untwisting. The results of such an experiment are shown in Fig. 5. A spun fiber with $P = 5$ cm which initially exhibited negligible retardance or rotation was untwisted and the measured linear-component of birefringence compared with calculation according to (8). At the point when the fiber was completely untwisted [i.e, when the reverse twist was $\xi_r = 2\pi/P(1 - g')$ in (8)], a linear birefringence $\delta\beta = 14.4°/$[m] reappeared, which is similar to the value $\delta\beta = 32°/$m measured in an unspun section 100 m down the fiber. We can conclude, therefore, that the spinning process leaves the local internal birefringence virtually unaltered.

Routine production of low-birefringence fibers from virtually any preform is now possible using the spinning technique. It is an advantage, however, to use a preform capable of giving fibers with $L_p > 1$ m, so that $P \simeq 10$ cm is required. No loss increase has been found at this spin pitch and the preform rotation rate (~600 r/min at a pulling speed of 1 m/s) is easily manageable.

IV. High-Birefringence Fibers

The quest for low-loss polarization-maintaining fibers with $L_p < 1$ mm has centered on 1) the use of highly elliptical cores to increase B_G [7] and 2) increasing the stress-induced anisotropy B_S [36]. More recently, a fiber with an axially nonsymmetric refractive-index distribution has been proposed [37] in which one of the linearly polarized modes is cut off while the other propagates. Although the structure is truly "single polarization," such behavior exists over a narrow wavelength range and the orthogonally polarized guided-mode is weakly bound, being itself close to cutoff. These problems could be obviated if it becomes possible to use higher values of relative index-difference Δ without incurring a loss penalty. However, the structure can also be used as a means of increasing $\delta\beta$ when both modes are propagating.

A. Shape-Birefringent Fibers

Returning to Fig. 2, we see that for values of $(a/b - 1) > 1$ the curve departs considerably from linearity and B_G is proportional to $(\Delta n)^2$, but no longer to $(a/b - 1)$, as was the case for small ellipticity. The curve is plotted using the results calculated in [38] and assumes operation at the higher mode cutoff, values for which are given in [39]. Note that the curve has an optimum $(a/b - 1) \sim 5$ which maximizes $B_G/(\Delta n)^2$, although little is to be gained by using $a/b > 3$. However, an increase in Δn is always advantageous, and, recognizing this, Dyott [38] has reported on a fiber consisting of a small GeO_2/SiO_2 core having $\Delta n = 0.065$ and $a/b = 2.5$ within a silica substrate. The fiber is marked on Fig. 1 and had L_p (0.633 μm) = 0.75 mm, which is close to the predicted value. An attempt in our laboratory to exploit both stress and shape birefringence by using an elliptical GeO_2/SiO_2 core and B_2O_3/SiO_2 cladding within a silica substrate produced a fiber (VD299) with $\Delta n = 0.35$, $a/b = 2.2$, and L_p (0.633 μm) = 2 mm. This fiber has $B_G/(\Delta n)^2 = 0.25$, which is above the curve in Fig. 1, indicating that stress contributed about 15 percent to the measured birefringence. The cross section of the fiber is shown in Fig. 2(b).

The refractive-index profile in the core of the preform from which a typical shape-birefringent fiber is drawn is shown in Fig. 6. The profile was measured by the spatial-filtering method [40] and uses a tomographic reconstruction technique [41]. This figure illustrates the high core ellipticity required in fibers of this type.

B. Side-Pit Fibers

The calculated value of $B_G/(\Delta n)^2$ is marked on Fig. 1 for side-pit fibers with $(a/b - 1) = 2.3$, and is approximately the same for the three values of pit depression given in [18]. Again we assume that the guide is operating at higher mode cutoff. Here we have taken Δn as the difference between the index level of the pit and that at the core center so as to provide a comparison with a conventional elliptical-core fiber with similar cladding depression. It can be seen that the side-pit fiber has $B_G/(\Delta n)^2 \sim 0.5$, i.e., about twice the birefringence of an equivalent elliptical-core fiber. Attempts to fabricate the structure [42] gave $B = 5 \times 10^{-5}$, (L_p(1.15 μm) = 23 mm), although it was acknowledged [43] that the fiber was dominated by stress birefringence. This discovery led to an interesting new stress-producing structure [43] which has given $B = 8.5 \times 10^{-5}$, (L_p(1.15 μm) = 13.5 mm), and a loss of 0.62 dB/km at 1.52 μm.

C. Fibers with Stress-Induced Anisotropy

The most successful approach to the fabrication of high-birefringence fibers has been to use the differential thermal expansion coefficients of the doped core/cladding structure relative to the silica substrate to increase the internal tensile stress to a value close to the elastic limit of the materials [44].

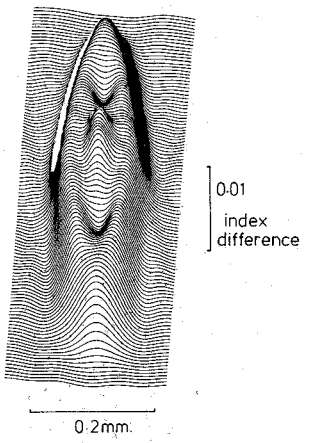

Fig. 6. Index profile [40], [41] of typical shape-birefringence preform showing high ellipticity.

In a simple analysis of a three-layer composite slab in which a thin core/cladding structure is sandwiched between thick silica substrate layers [45], the stress birefringence B_S is given by

$$B_S = -EC(\alpha_1 - \alpha_2)(T_1 - T_0). \tag{13}$$

Here α_1 and α_2 are the expansion coefficients of the core/cladding structure and substrate, respectively, and T_1 and T_0 are the core/cladding fictive temperature and room temperature.

Note that in (13) we have used T_1 for the core material and not for the substrate. Although the substrate usually sets at several hundred °C higher than the core, in the temperature interval between their respective setting points the core is liquid and experiences only hydrostatic pressure as it contracts within the solid substrate. Thus, the core cannot support anisotropic stresses until it in turn sets. Therefore, it is thought that viscoelastic stresses do not play a significant part in fiber birefringence, although they contribute substantially to overall fiber stresses [46].

The present state of the art in low-loss stress-birefringent fibers can be seen in a report by Katsuyama *et al.* [47]. The fiber [cross section shown in Fig. 2(c)] has an elliptical, highly doped stress-producing structure, within which is a circular, lightly doped core. The core is optically buffered from the elliptical cladding by an undoped silica annulus. The fiber had (L_p(0.633 μm) = 2 mm) and a loss of 0.8 dB/km at 1.55 μm. More recently a fiber with the same loss and (L_p(0.633 μm) = 0.87 mm) has been obtained [48]. These fibers are reported to have a polarization extinction ratio of >30 dB in a 500 m length [47] wound on a 30 cm drum. The fiber is marked on Fig. 1 to demonstrate how the constraints of shape birefringence can be circumvented by the use of stress.

In Table I a comparison is made between polarization-maintaining fibers using either shape or stress birefringence, these being the most common approaches. Shape-birefringent fibers have yet to demonstrate low loss, although this is not thought to be an inherent limitation caused by the high values of Δ required, as demonstrated by reports of low-loss multimode fibers with Δ = 2.4 percent [49].

Since stress-birefringent fibers are now operating close to the fracture point of the materials, it would appear that a further increase in birefringence can only be obtained by resorting to combinations of stress and shape birefringence, or the development of new waveguiding structures. For example, multimode stress-birefringent fibers have recently been reported [50].

D. Circularly Birefringent Fibers

As we have seen (Section III-B), twisting results in a reduction in the net linear-birefringence of a fiber. If a linearly birefringent fiber is highly twisted such that $(\xi - \alpha) \gg \delta\beta$, the internal birefringence $\delta\beta$ can be almost completely eliminated in much the same way as in a spun fiber. However, in contrast with a spun fiber, a twisted fiber retains a relatively large torsion-induced circular birefringence, given from (9) by

$$\Omega(z) = \alpha z \tag{14}$$

which is identical to (4). Thus, provided that the twist is sufficiently large, the fiber internal linear-birefringence can be completely substituted by circular birefringence. The elliptically polarized modes of the slightly twisted fiber (Section II-C) become circularly polarized for $(\xi - \alpha) \gg \delta\beta$ and have a difference in propagation constants $\delta\beta_{\text{circ}} = 2g'\xi$. By contrast, the spun fiber has circularly polarized modes which are nearly degenerate.

A highly twisted fiber maintains circular polarization in the same way that a linearly birefringent fiber preserves linear polarization [22]; a circularly polarized input state will not couple to its opposite-handed counterpart provided $\delta\beta_{\text{circ}}$ can be made large compared to the birefringence induced by external perturbations. This fact forms the basis of a proposal [51] to employ highly twisted fibers in a circular-polarization maintaining fiber-cable design. The particular advantage of the approach is that angular orientation of the fibers at joints is not required, whereas in linearly birefringent fibers, failure to align the birefringent axes of the fibers causes excitation of the unwanted mode. It has been calculated [52] that an rms misalignment of less than 3.6° must be achieved when joining 25 sections of linear polarization-maintaining fiber in order to keep the unwanted mode power below 10 percent.

A practical maximum twist-rate for a cabled fiber is about 50 twists/m. From (4) we have a normalized circular-birefringence $B_{\text{circ}}(1.3\ \mu\text{m}) = 9.5 \times 10^{-6}$ and therefore a mode beat-length L_p = 13.7 cm is achievable.

V. Performance of Polarization-Maintaining Fibers

The ability of a high-birefringence fiber to sustain a polarization state depends on the magnitude and spatial period of the birefringence induced by external factors. In any real installation, bends, transverse pressure, and twists will be random in nature and an analysis of their effect therefore depends upon a statistical knowledge of the perturbation distributions likely to be met in a given cable design [17]. Such information is not easily obtainable and, moreover, the analysis is tedious. We can, however, calculate the effect of single bends and twists to provide a comparison between the polarization-holding performance of various high-birefringence fibers. The results provide an indication of the criteria to be met when designing a protective cable structure.

When a linearly or circularly birefringent fiber is subjected to

TABLE I
COMPARISON OF STRESS AND SHAPE-BIREFRINGENT POLARIZATION-MAINTAINING FIBERS

	Stress-Birefringent Fibres	Shape-birefringent fibres
Attenuation	Low (0.8dB/km @ 1.55μm [47])	High at present (~ 40dB/km)
Core geometry	Circular [36], [43], [47] or elliptical [7] with dimensions similar to conventional fibres.	Highly elliptical and small [38]. Typically 3μm x 1μm for λ = 1μm operation
Effect of temperature on birefringence	High [29]	Low
Polarisation mode-dispersion	High (up to 2ns/km)	Can possibly be equalised [38]
Reduction of birefringence with age	Some reported [36] None observed [48]	Not expected

a bend or twist, coupling is produced between the normal modes of the unperturbed fiber and results in power interchange. The energy periodically found in the unwanted mode can be calculated by coupled mode theory; alternatively, we can gain some insight into the problem by regarding it in terms of interspersed retarder and rotator birefringent-elements at a suitable orientation to one another to account for the direction of the applied perturbation [24], [53]. Thus, a linear-polarization maintaining fiber subject to a bend (or transverse pressure) can be modeled as a series of retarder plates representing the fiber, interspersed with further retarder plates representing the bend birefringence. The latter have axes orientated within the plane of the bend. Similarly, a linear-polarization maintaining fiber subject to twist is modeled as a series of precessing retarder-plates interleaved with rotator elements representing the twist, while a circular-polarization maintaining fiber subject to a bend is a series of rotators alternating with retarders at the fixed orientation of the bend. In all three cases we follow the procedure outlined in [53] to calculate the extinction ratio $\epsilon(z)$, the ratio of power in the unwanted mode to that in the desired mode,

$$\epsilon(z) = \frac{q_i^2 \sin^2 \gamma_i z}{1 + q_i^2 \cos^2 \gamma_i z} \tag{15}$$

where q_i, γ_i refer to the above three cases.

A. Linear-Polarization Maintaining Fiber with Bend

A linearly birefringent fiber with birefringence $\delta\beta$ subject to a bend (or transverse pressure) having birefringence $\delta\beta_B$ in a plane orientated at angle θ to the fiber principal axes has q and γ in (15) given by

$$q = \frac{\delta\beta_B \sin 2\theta}{\delta\beta}; \quad \gamma = \frac{1}{2}(\delta\beta^2 + \delta\beta_B^2 \sin^2 2\theta)^{1/2}. \tag{16}$$

The extinction ratio $\epsilon(z)$ oscillates along the length of the bent fiber and positions can be found at which all power has returned to the original polarized mode (i.e., $\epsilon(z) = 0$). These points occur for small $\delta\beta_B$ at $z \simeq 2\pi N/\delta\beta = NL_p$, where N is an integer. Thus, testing a fiber for polarization-holding ability by wrapping it around a mandril, as is frequently done, can lead to optimistic results, since $\epsilon(z)$ depends on both the orientation θ of the bend and its length. It is possible for several meters of fiber to be tightly coiled and exhibit excellent polarization-holding ability if 1) the plane of the bend is parallel to one of the fiber principal axes ($\theta = 0, \pi/2$) or 2) the wrapped length is a multiple of L_p.

The poorest extinction ratio $\epsilon_{\min} = q^2$ occurs for small $\delta\beta$ at $z \simeq (1 + 2N)\ \pi/\delta\beta$, i.e., periodically at intervals of L_p which alternate with the points of high extinction ratio. The maximum power transfer occurs when the period of the perturbation, in this case a bend, is equal to a multiple of L_p, a criterion which corresponds to the well-known coupled-mode theory condition for maximum coupling.

$\epsilon_{\min}$ is plotted in Fig. 7 using (15), (16) for a 125 μm diameter fiber having L_p(1.3 μm) = 2, 10, and 30 mm as a function of bend radius, with the bend applied at $\theta = 45°$. We see that even for the $L_p = 2$ mm fiber, a bend of 5 mm radius degrades the extinction ratio to -30 dB. The length of the bend need only be $L_p/2 = 1$ mm.

B. Linear-Polarization Maintaining Fiber with Twist

For a linearly birefringent fiber having birefringence $\delta\beta$ subject to a small twist of ξ rads/m, q and γ in (15) are given by

$$q = \frac{2\xi(1 - g')}{\delta\beta}; \quad \gamma = \frac{1}{2}[\delta\beta^2 + (2\xi(1 - g'))^2]^{1/2}. \tag{17}$$

Note that this is the same case as treated in Section III-B and yields identical values for q and γ.

$\epsilon(z)$ is again oscillatory with length and $\epsilon_{\min}$ occurs at multiples of L_p. Fig. 7 shows $\epsilon_{\min}$ as a function of twist for fibers having L_p(1.3 μm) = 2, 10, 30 mm and we see that for a fiber with $L_p = 2$ mm, a twist of 8 turns/m is sufficient to degrade the extinction ratio to -31 dB.

C. Circular-Polarization Maintaining Fiber

A fiber deliberately twisted at a rate ξ rads/m to induce high circular-birefringence when subject to a bend having birefringence $\delta\beta_B$ gives

$$q = \frac{\delta\beta_B}{2g'\xi}; \quad \gamma = \frac{1}{2}[\delta\beta_B^2 + (2g'\xi)^2]^{1/2}. \tag{18}$$

In this case the fiber is particularly sensitive to bends, since

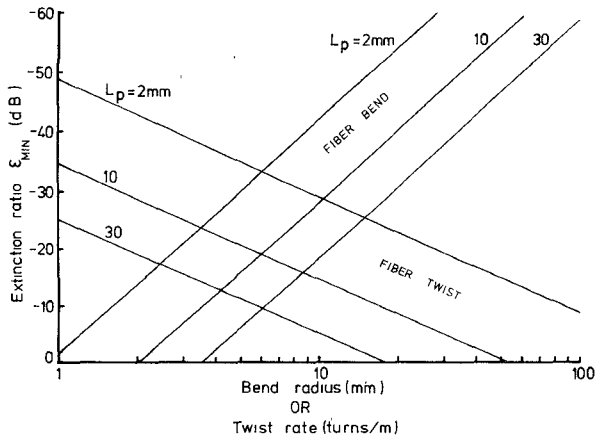

Fig. 7. Minimum extinction ratio ϵ_{min} for linear-polarization maintaining fibers subject to bends or twists, shown for various values of L_p (1.3 μm). Fibers are 125 μm in diameter.

for a 125 μm fiber twisted at 50 turns/m, a bend of only 45 mm radius degrades ϵ_{min} to - 31 dB (λ = 1.3 μm).

It is clear that under certain conditions relatively gentle bends and twists can significantly affect the extinction ratio, even in fibers with small values of L_p. Thus, if high extinction ratios are to be maintained in long lengths then some care in fiber packaging will be needed to avoid, in particular, quite minor microbends. From the examples given above it would appear necessary to avoid microbends with a radius of less than ~5 mm for a linear-polarization maintaining fiber and less than 45 mm for a circular-polarization maintaining fiber. Further information on the statistics of cabled fiber perturbations is required before realistic estimates of polarization performance can be made. It may be that when long lengths are involved, active stabilization of the fiber output polarization [54], [55] is a preferable solution.

We note in passing that (15)-(18) can be used to show how internal fiber birefringence limits the sensitivity of polarimetric sensors which rely on externally induced birefringence. Take, for example, a magnetic-field detector [8], [11] in which the Faraday effect produces a rotation α_F per unit length. The magnetic field can be measured by observing the power transferred into the mode orthogonal to that excited, by means of an analyzer at the fiber output. Since we are interested in unidirectional propagation, Faraday rotation is indistinguishable from elastooptic rotation and the term $\xi(1 - g')$ can be replaced in (17) by α_F. Then for small α_F, the maximum power which can be detected in the orthogonal mode occurs for a fiber length of $L_p/2$ and is $\epsilon_{min} = 4\alpha_F^2/\delta\beta^2$. Thus, the longest usable fiber interaction length is limited to $L_p/2$, making a low-birefringence fiber attractive for applications which require several meters of fiber to surround a current-carrying conductor [8], [9]. Furthermore, the sensor calibration is dependent on $\delta\beta$, which is temperature sensitive in all but very low birefringence and spun fibers.

VI. Polarization Mode-Dispersion

By balancing waveguide and material dispersion, single-mode fibers can be designed with small total chromatic dispersion over the full wavelength region 1.3-1.7 μm [56]-[58], leaving only polarization mode-dispersion as a potential bandwidth-limiting factor [16], [59]. We consider here the source and magnitude of the effect.

A. Linearly Birefringent Fibers

If both orthogonally polarized modes are excited, the presence in the fiber of shape and stress birefringence B_G and B_S leads to a group-delay difference $\Delta\tau$ given by the derivative of the birefringence $\delta\beta$ with respect to k, the free-space wave number:

$$\Delta\tau = \frac{L}{c}\frac{d(\delta\beta)}{dk} = \frac{L}{c}\frac{d}{dk}\left[k(B_G + B_S)\right]$$
$$= \frac{L}{c}\left[B_G + k\frac{dB_G}{dk} + B_S\left(1 + \frac{k}{C}\frac{dC}{dk}\right)\right] \quad (19)$$

where L is the fiber length, c is the velocity of light, and C is the stress-optical coefficient. The dispersion in the latter [60] [i.e., the final term in (19)] contributes about 5 percent to the dispersion due to B_S and is usually neglected.

A polarization-dispersion curve (Fig. 8) calculated as a function of V from (19) for a typical telecommunications fiber illustrates the relative contributions of shape and stress birefringence. We have taken $B_S = 7.7 \times 10^{-7}$ and calculated the waveguide shape component ($B_G + k\,dB_G/dk$) using the well established polarization-dispersion formula for step-index elliptical fibers [32] with Δ = 0.5 percent and an ellipticity $(1 - a/b) = 4$ percent. The values of B_S and ellipticity were chosen to fit data (dots) obtained in an experiment, and will be described in a subsequent section. From Fig. 8 we see that near the higher mode cutoff (V = 2.4) the waveguide shape dispersion is small and vanishes at V = 2.47, leaving only the stress component LB_S/c.

Since operation at V-values close to 2.4 is usual in fibers designed for the 1.3 μm wavelength region, the waveguide polarization-dispersion component is normally negligible. This may not be the case in fibers for the 1.5 μm region [16], [59], where lower V-values are necessary to obtain zero total chromatic dispersion [56]. Nevertheless, for most types of fiber and for stress-birefringent polarization-maintaining fibers stress is the dominant factor and $\Delta\tau \simeq LB_S/c$. In the latter fibers relatively large $\Delta\tau$ can arise from their high birefringence if energy transfers to the unwanted mode. For example, in a fiber with L_p(1.3 μm) = 2 mm we calculate $\Delta\tau$ = 2.2 ns/km. A measurement at 815 nm on 1.87 km of high-birefringence fiber gave only ~0.1 ns/km [61], although it is probable that L_p in this fiber was much larger than the 2 mm of our example. Nevertheless, the measurement shows that the bandwidth in high-birefringence fibers can be severely limited if the unwanted mode is excited by bends, twists, and joints [52].

Owing to its small value, $\Delta\tau$ is difficult to measure directly in the time domain, except in high-birefringence fibers. We can, however, resort to a measurement of $\delta\beta$ as a function of wavelength, and obtain $\Delta\tau$ from the derivative, according to (19). Using this method [62], the individual contributions of shape and stress birefringence have been estimated and a value for B_S which corresponds to $\Delta\tau$ = 50 ps/km found in a fiber with an ellipticity of 0.35. However, for long fiber lengths in which random mode-coupling dominates, some difficulty is experienced, as indicated in [63]. The reason is that (19) requires the variation with wavelength of the normal modes of the fiber to determine $\Delta\tau$, and these can only be defined on a local scale in a fiber with random mode-coupling. Measurements of the output polarization state do not define nor-

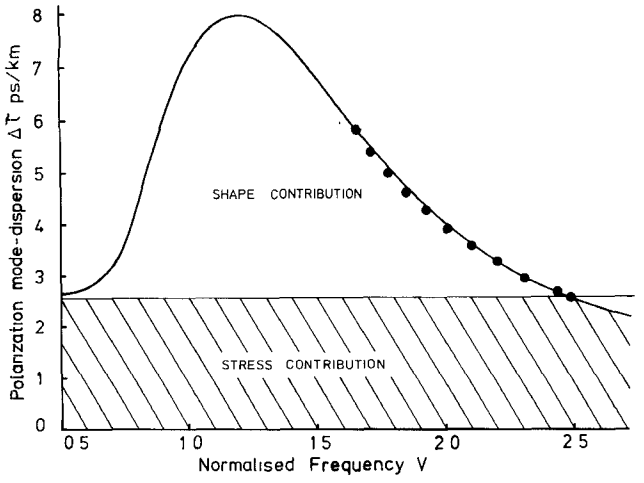

Fig. 8. Calculated polarization mode-dispersion in a fiber with $B_S = 7.7 \times 10^{-7}$, ellipticity $(1 - a/b) = 4$ percent, $\Delta = 0.5$ percent, showing relative contributions of stress and shape birefringence. Dots are experimental points calculated using the results of Fig. 9.

mal modes, except in fibers with length-invariant properties.

Measurements of $\Delta\tau$ have also been made by methods which observe the coherence between the two modes of the fiber, either as a function of source spectral-width [64], or by compensating the delay difference between the modes within the two arms of an interferometer [65], [66]. The measurements reported in [63] and [65] were made on long lengths of telecommunications-grade fibers and less than 1 ps/km was found. Both measurements indicate that mode coupling had occurred. By contrast, the value for $\Delta\tau$ determined in [66] for a 1.02 km fiber with high stress-anisotropy was 188 ps/km.

B. Twisted and Spun Fibers

A twisted or spun linearly birefringent fiber can be regarded as a waveguide in which the two linearly polarized modes of the untwisted fiber are uniformly coupled and thus exchange power along the length. However, in the case of random mode-coupling, only local normal-modes can be defined, whereas when uniform mode-coupling is present, we can redefine our system of coordinates to one in which the modes are length invariant. They are thus the normal modes of the fiber [22], [24]. For a twisted fiber the required coordinate axes rotate with the twist. Since we now have well-defined normal modes, we have no difficulty in calculating the polarization mode-dispersion in terms of 2γ, the difference in propagation constant between them,

$$\Delta\tau = \frac{L}{c}\frac{d(2\gamma)}{dk} \tag{20}$$

where γ was first introduced in Section III and is given by (11). We now see that 2γ is simply the difference in propagation constant between the normal modes of the perturbed fiber, which in the case of a twisted fiber are elliptically polarized. From (11) and (20)

$$\Delta\tau = \frac{q}{(1+q^2)^{1/2}}\left(\frac{\Delta\tau_0}{q} - \frac{2L}{c}\frac{\alpha n}{C}\frac{d(C/n)}{dk}\right) \tag{21}$$

where q is given in (10). Again we have included the dispersion of the stress-optic coefficient C. $\Delta\tau_0$ is the dispersion of the fiber without twist and is given by (19). For a spun fiber $\alpha = 0$, and, if the spin rate is high, i.e., $\xi \gg \delta\beta$, (21) reduces to [23]

$$\Delta\tau = \frac{\delta\beta}{2\xi}\Delta\tau_0. \tag{22}$$

Thus, spinning the preform to produce a low-birefringence fiber has the considerable additional advantage that the polarization mode-dispersion is reduced in inverse proportion to the spin rate and can be made negligibly small. Spin rates of up to 2000 r/min have been achieved [34], which at a pulling speed of 1 m/s gives a spin pitch of $P = 3$ cm. Taking the criterion that we require $L_p > 50$ m for ultrahigh bandwidth transmission systems [16], we see from (22) that this can be achieved provided the fiber has an unspun $L_p > 0.9$ m. The latter figure can be met without particular care in manufacturing.

Experimental confirmation of the considerable reduction in polarization mode-dispersion obtainable by fiber spinning is given in Fig. 9. Here the variation of birefringence with wavelength, measured using two polarizers and a Soleil compensator, is plotted for both a spun and unspun section of the same fiber. Since we require the wavelength variation of the normal modes to calculate $\Delta\tau$ according to (19) and (21), linear birefringence was measured in the unspun fiber and circular in the spun section, although in the latter fiber negligible linear or circular birefringence was found.

From the curve of Fig. 9 the polarization mode-dispersion of the unspun fiber can be calculated as a function of V using (19). The results are superimposed on the theoretical curve of Fig. 8 which, as already indicated, was chosen as the best fit to the data. We can infer from the close correlation between the curves that this particular fiber had $B_S \simeq 7.7 \times 10^{-7}$, being the value which corresponds to $\Delta\tau = 2.6$ ps/km at $V = 2.47$, where the waveguide shape component is zero. The shape contribution is determined from the variation of $\Delta\tau$ with wavelength, from which we calculate a core ellipticity of ~4 percent. This agrees well with the measured value of ~3 percent. We have not plotted the value of $\Delta\tau$ for the spun fiber section, since no measurable change in birefringence with wavelength was found (Fig. 9) and consequently $\Delta\tau < 0.1$ ps/km (an equivalent $L_p(1.3\ \mu\text{m})$ of >40 m). Thus, spinning the fiber has reduced $\Delta\tau$ from a value of 5.2 ps/km at 1.3 μm ($V = 1.77$) in the unspun section to an immeasurably small value.

A similar reduction in $\Delta\tau$ occurs for a fiber twisted after drawing [67]. However, in this case the dispersion of the stress-optical coefficient C becomes significant. Using (21), we calculate from the data of [60] and our own measurements of $d(C/n)/d\lambda$ that a twist of 100 turns/m gives $\Delta\tau(1.3\ \mu\text{m}) \simeq 5$ ps/km between circularly polarized modes.

The role of random mode-coupling in reducing $\Delta\tau$ in long cabled fiber lengths is not at present clear. Further study on the natural spectrum of bends and twists likely to be encountered is required before a realistic prediction can be made.

The effect of polarization mode-dispersion may be summarized as follows.

1) Energy transfer between modes in linear-polarization maintaining fibers produces significant polarization dispersion unless steps are taken to filter out the unwanted mode.

2) Telecommunications-grade fibers have $\Delta\tau$ of the order of 5 ps/km, although in long lengths this is likely to be reduced by random mode-coupling.

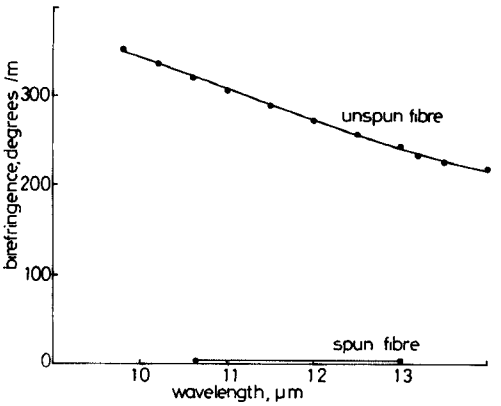

Fig. 9. Measured variation of birefringence with wavelength in spun and unspun sections of a fiber with $\lambda_{cutoff} = 0.96$ μm and equivalent step $\Delta = 0.5$ percent.

3) Polarization dispersion can be virtually eliminated by deliberately introducing uniform mode-coupling using fiber spinning.

VII. Conclusions

The ease with which the polarization properties of an optical fiber can be modified by external effects is actively being exploited in several sensor devices, while at the same time proving troublesome in applications which require a steady, defined polarization state. We have outlined the progress which has been made in developing both low and high-birefringence fibers with a view to respectively enhancing or suppressing environmental influences. A technique in which the internal birefringence can be all but eliminated by a process of spinning during drawing provides a solution to the routine production of low-birefringence fibers. At the other extreme, high-birefringence fibers with both low loss and good polarization-holding properties in lengths of 500 m have been reported.

An analysis of the effect of bends and twists on the performance of polarization-maintaining fibers shows that relatively minor perturbations can significantly degrade the extinction ratio. It is clear that care will be required in packaging the fibers if high extinction ratios are required over lengths of several kilometers. There is insufficient data available at present on the spectrum of perturbations to be found in a cabled fiber to translate laboratory measurements of polarization-holding ability into practical performance. It is foreseen that performance improvements will be made by careful design of a protective structure for the fiber.

A number of measurements of polarization mode-dispersion have now been reported and range from 200 ps/km in high-birefringence fibers to less than 1 ps/km in telecommunications-grade fibers. The role of natural mode-coupling in the fibers which produced the latter figures has yet to be determined. In fibers with significant polarization mode dispersion, fiber spinning can be used to provide uniform mode-coupling, which reduces the dispersion to a negligible level.

Acknowledgment

The authors would like to acknowledge R. Calligaro and R. D. Birch for their work on low- and high-birefringence fibers, respectively, and M. J. Adams for his valuable comments on the manuscript.

References

[1] R. Ulrich and M. Johnson, "Fiber-ring interferometer: Polarisation analysis," *Opt. Lett.*, vol. 4, pp. 152–154, 1979.
[2] G. Schiffner, W. R. Leeb, H. Krammer, and J. Wittman, "Reciprocity of birefringent single-mode fibers for optical gyros," *Appl. Opt.*, vol. 18, pp. 2096–2097, 1979.
[3] S. K. Sheem and T. G. Giallorenzi, "Polarisation effects on single-mode optical fiber sensors," *Appl. Phys. Lett.*, vol. 35, pp. 914–917, 1979.
[4] R. Ulrich, "Fiber-optic rotation sensing with low drift," *Opt. Lett.*, vol. 5, pp. 173–175, 1980.
[5] R. A. Steinberg and T. G. Giallorenzi, "Performance limitations imposed on optical waveguide switches and modulators by polarisation," *Appl. Opt.*, vol. 15, pp. 2440–2453, 1976.
[6] Y. Yamamoto and T. Kimura, "Coherent optical fiber transmission systems," *IEEE J. Quantum Electron.*, vol. QE-17, pp. 919–935, June 1981; and F. Favre, L. Jeunhomme, I. Joindot, M. Monerie, and J. C. Simon, "Progress towards heterodyne-type single-mode fiber communication systems," *IEEE J. Quantum Electron.*, vol. QE-17, pp. 897–906, June 1981.
[7] V. Ramaswamy, W. G. French, and R. D. Standley, "Polarisation characteristics of noncircular core single-mode fibers," *Appl. Opt.*, vol. 17, pp. 3014–3017, 1978.
[8] A. M. Smith, "Polarisation and magneto-optical properties of single-mode optical fibres," *Appl. Opt.*, vol. 17, pp. 52–56, 1978.
[9] A. Papp and H. Harms, "Faraday effect in glass fibers," *J. Magnetism Magnetic Materials*, vol. 2, pp. 287–291, 1976; and —, "Magneto-optical current transformer. Parts I–III," *Appl. Opt.*, pp. 3729–3745, 1980.
[10] S. C. Rashleigh, "Magnetic-field sensing with a single-mode fiber," *Opt. Lett.*, vol. 6, pp. 19–21, 1981; —, "Acoustic sensing with a single coiled monomode fiber," *Opt. Lett.*, vol. 5, pp. 392–394, 1980.
[11] H. Harms, A. Papp, and K. Kempter, "Magneto-optical properties of index-gradient optical fibers," *Appl. Opt.*, vol. 15, pp. 799–801, 1976.
[12] R. H. Stolen and E. H. Turner, "Faraday rotation in highly birefringent optical fibers," *Appl. Opt.*, vol. 19, pp. 842–845, 1980.
[13] Y. Yen and R. Ulrich, "Birefringent optical filters in single-mode fiber," *Opt. Lett.*, vol. 6, pp. 278–280, 1981.
[14] H. C. Lefevre, "Single-mode fibre fractional wave devices and polarisation controllers," *Electron. Lett.*, vol. 16, pp. 778–780, 1980.
[15] M. Johnson, "Single-mode-fiber birefringent filters," *Opt. Lett.*, vol. 5, pp. 142–144, 1980.
[16] D. Marcuse and C. Lin, "Low dispersion single-mode fiber transmission–The question of practical versus theoretical maximum transmission bandwidth," *IEEE J. Quantum Electron.*, vol. QE-17, pp. 869–878, June 1981.
[17] I. P. Kaminow, "Polarization in optical fibers," *IEEE J. Quantum Electron.*, vol. QE-17, pp. 15–22, Jan. 1981.
[18] T. Okoshi, "Single-polarization single-mode optical fibers," *IEEE J. Quantum Electron.*, vol. QE-17, 1981.
[19] F. P. Kapron, N. F. Borrelli, and D. B. Keck, "Birefringence in dielectric optical waveguides," *IEEE J. Quantum Electron.*, vol. QE-8, pp. 222–225, 1972.

[20] D. Marcuse, *Theory of Dielectric Optical Waveguides*. New York: Academic, 1974.
[21] A. Papp and H. Harms, "Polarisation optics of index-gradient optical waveguide fibers," *Appl. Opt.*, vol. 14, pp. 2406–2411, 1975.
[22] R. Ulrich and A. Simon, "Polarisation optics of twisted single-mode fibers," *Appl. Opt.*, vol. 18, pp. 2241–2251, 1979.
[23] A. J. Barlow, J. J. Ramskov Hansen, and D. N. Payne, "Birefringence and polarisation mode-dispersion in spun single-mode fibers," *Appl. Opt.*, vol. 20, pp. 2962–2968, 1981.
[24] P. McIntyre and A. W. Snyder, "Light propagation in twisted anisotropic media: Application to photo receptors," *J. Opt. Soc. Amer.*, vol. 68, pp. 149–157, 1978.
[25] R. Ulrich, S. C. Rashleigh, and W. Eickhoff, "Bending-induced birefringence in single-mode fibers," *Opt. Lett.*, vol. 5, pp. 273–275, 1980.
[26] A. M. Smith, "Single-mode fibre pressure sensitivity," *Electron. Lett.*, vol. 16, pp. 773–774, 1980 (note that this reference seems to have used silica constants which give a rather high value for C).
[27] J. Sakai and T. Kimura, "Birefringence and polarization characteristics of single-mode optical fibers under elastic deformations," *IEEE J. Quantum Electron.*, vol. QE-17, pp. 1041–1051, June 1981.
[28] W. A. Gambling, D. N. Payne, and H. Matsumura, "Birefringence and optical activity in single-mode fibres," presented at the Top. Meet. on Opt. Fiber Transmission II, Williamsburg, VA, 1977, paper TuD5-1.
[29] V. Ramaswamy, R. H. Stolen, M. D. Divino, and W. Pleibel, "Birefringence in elliptically clad borosilicate single-mode fibers," *Appl. Opt.*, vol. 18, pp. 4080–4084, 1979.
[30] H. Schneider, H. Harms, A. Papp, and H. Aulich, "Low-birefringence in single-mode optical fibers: Preparation and polarisation characteristics," *Appl. Opt.*, vol. 17, pp. 3035–3037, 1978.
[31] S. R. Norman, D. N. Payne, M. J. Adams, and A. M. Smith, "Fabrication of single-mode fibres exhibiting extremely low polarisation birefringence," *Electron. Lett.*, vol. 15, pp. 309–311, 1979.
[32] M. J. Adams, *An Introduction to Optical Waveguides*. Chichester: Wiley, 1981.
[33] S. C. Rashleigh and R. Ulrich, "Magneto-optic current sensing with birefringent fibers," *Appl. Phys. Lett.*, vol. 34, pp. 768–770, 1979.
[34] A. J. Barlow, D. N. Payne, M. R. Hadley, and R. J. Mansfield, "Production of single-mode fibres with negligible intrinsic birefringence and polarisation mode dispersion," *Electron. Lett.*, vol. 17, pp. 725–726, 1981.
[35] A. Ashkin, J. M. Dziedzic, and R. H. Stolen, "Outer diameter measurement of low birefringence optical fibers by a new resonant backscatter technique," *Appl. Opt.*, vol. 20, pp. 2299–2303, 1981.
[36] R. H. Stolen, V. Ramaswamy, P. Kaiser, and W. Pleibel, "Linear polarisation in birefringent single-mode fibers," *Appl. Phys. Lett.*, vol. 33, pp. 699–701, 1978.
[37] T. Okoshi and Y. Oyamada, "Single-polarisation single-mode optical fibre with refractive-index pits on both sides of core," *Electron. Lett.*, vol. 16, pp. 712–713, 1980.
[38] R. B. Dyott, J. R. Cozens, and D. G. Morris, "Preservation of polarisation in optical-fibre waveguides with elliptical cores," *Electron. Lett.*, vol. 15, pp. 380–382, 1979; also private communication.
[39] S. R. Rengarajan and J. E. Lewis, "First higher-mode cut off in two-layer elliptical fibre waveguides," *Electron. Lett.*, vol. 16, pp. 263–264, 1980.
[40] I. Sasaki, D. N. Payne, and M. J. Adams, "Measurement of refractive-index profiles in optical-fibre preforms by spatial filtering technique," *Electron. Lett.*, vol. 16, pp. 219–221, 1980.
[41] P. L. Francois, I. Sasaki, and M. J. Adams, "Practical three-dimensional profiling of optical fiber preforms," *IEEE J. Quantum Electron.*, this issue, pp. 524–534.
[42] T. Hosaka, K. Okamoto, Y. Sasaki, and T. Edahiro, "Single-mode fibres with asymmetrical refractive index pits on both sides of core," *Electron. Lett.*, vol. 17, pp. 191–193, 1981.
[43] T. Hosaka, K. Okamoto, T. Miya, Y. Sasaki, and T. Edahiro, "Low-loss single polarisation fibres with asymmetrical strain birefringence," *Electron. Lett.*, vol. 17, pp. 530–531, 1981.
[44] For a review of the development of stress-birefringent fibers, see [17].
[45] I. P. Kaminov and V. Ramaswamy, "Single-polarisation optical fibers: Slab model," *Appl. Phys. Lett.*, vol. 34, pp. 268–270, 1979.
[46] G. W. Scherer and A. R. Cooper, "Thermal stresses in clad-glass fibers," *J. Amer. Ceramic Soc.*, vol. 63, pp. 346–347, 1980.
[47] T. Katsuyama, H. Matsumura, and T. Suganuma, "Low-loss single-polarisation fibres," *Electron. Lett.*, vol. 17, pp. 473–474, 1981.
[48] H. Matsumura, private communication.
[49] N. Shibata, M. Kawachi, S. Suda, and T. Edahiro, "Low-loss high-numerical-aperture optical fibre fabricated by VAD method," *Electron. Lett.*, vol. 15, pp. 680–681, 1979.
[50] R. E. Wagner, R. H. Stolen, and W. Pleibel, "Polarisation preservation in multimode fibers," *Electron. Lett.*, vol. 17, pp. 177–178, 1981.
[51] L. Jeunhomme and M. Monerie, "Polarisation-maintaining single-mode fibre cable design," *Electron. Lett.*, vol. 16, pp. 921–922, 1980.
[52] M. Monerie, "Polarisation-maintaining single-mode fibre cables: Influence of joints," *Appl. Opt.*, vol. 20, pp. 2400–2406, 1981.
[53] A. J. Barlow and D. N. Payne, "Polarisation-maintenance in circularly birefringent fibres," *Electron. Lett.*, vol. 17, pp. 388–389, 1981.
[54] R. Ulrich, "Polarisation stabilisation on single mode fiber," *Appl. Phys. Lett.*, vol. 35, pp. 840–842, 1979.
[55] M. Kubota, T. Oohara, K. Furuya, and Y. Suematsu, "Electro-optical polarisation control on single-mode optical fibres," *Electron. Lett.*, vol. 16, pp. 573–574, 1980.
[56] W. A. Gambling, H. Matsumura, and C. M. Ragdale, "Mode dispersion, material dispersion and profile dispersion in graded-index single-mode fibers," *IEE J. Microwaves, Opt., Acoust.*, vol. 3, pp. 239–246, 1979; and —, "Zero total dispersion in graded-index single-mode fibres," *Electron. Lett.*, vol. 15, pp. 474–476, 1979.
[57] L. G. Cohen, C. Lin, and W. G. French, "Tailoring zero chromatic dispersion into the 1.5–1.6 μm low-loss spectral region of single-mode fibres," *Electron. Lett.*, vol. 15, pp. 334–335, 1979.
[58] T. Mya, K. Okamoto, Y. Ohmori, and Y. Sasaki, "Fabrication of low-dispersion single-mode fibers over a wide spectral range," *IEEE J. Quantum Electron.*, vol. QE-17, pp. 858–861, June 1981.
[59] H. Tsuchiya and N. Imoto, "Dispersion-free single-mode fibre in 1.5 μm wavelength region," *Electron. Lett.*, vol. 15, pp. 476–478, 1979.
[60] N. K. Sinha, "Normalised dispersion of birefringence of quartz and stress optical coefficient of fused silica and plate glass," *Phys. Chem. Glasses*, vol. 19, pp. 69–77, 1978.
[61] M. Monerie, P. Lamouler, and L. Jeunhomme, "Polarisation mode-dispersion measurements in long single-mode fibres," *Electron. Lett.*, vol. 16, pp. 907–908, 1980.
[62] N. Imoto, N. Yoshizawa, J. Sakai, and H. Tsuchiya, "Birefringence in single-mode optical fiber due to elliptical core deformation and stress anisotropy," *IEEE J. Quantum Electron.*, vol. QE-16, pp. 1267–1271, 1980.
[63] N. Imoto and M. Ikeda, "Polarization dispersion measurement in long single-mode fibers with zero dispersion wavelength at 1.5 μm," *IEEE J. Quantum Electron.*, vol. QE-17, pp. 542–545, June 1981.
[64] S. C. Rashleigh and R. Ulrich, "Polarisation mode dispersion in single-mode fibres," *Opt. Lett.*, vol. 3, pp. 60–62, 1978.
[65] K. Mochizuki, Y. Namihira, and K. Wakabayashi, "Polarisation mode dispersion measurements in long single mode fibres," *Electron. Lett.*, vol. 17, pp. 153–154, 1981.
[66] N. Shibata, M. Tateda, S. Seikai, and N. Uchida, "Wavelength dependence of polarisation mode dispersion in elliptical-core single-mode fibres," *Electron. Lett.*, vol. 17, pp. 564–565, 1981.
[67] M. Monerie and L. Jeunhomme, "Polarisation mode coupling in long single mode fibers," *Opt. Quantum Electron.*, vol. 12, pp. 449–461, 1980.

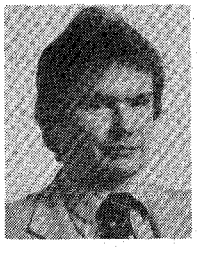

David N. Payne was born in Lewes, England, on August 13, 1944 and educated in Central Africa. He received the B.Sc. degree in electrical engineering, the Diploma in quantum electronics, and the Ph.D. degree from the University of Southampton, Southampton, England.

In 1972 he became the Pirelli Research Fellow in the Department of Electronics, University of Southampton and in 1977 he was appointed to the Optical Communications Group as a Senior Research Fellow. Since 1969 his research interests have been in optical communications and have included preform and fiber fabrication techniques, optical propagation in multimode and single-mode fibers, fiber and preform characterization, wavelength-dispersive properties of optical fiber materials, optical transmission measurements, and fiber devices. Currently, his main fields of interest are polarization properties of optical fibers, fiber sensors, and optical transmission.

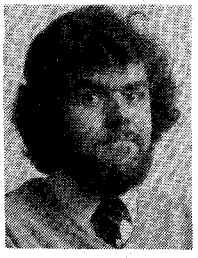

Arthur J. Barlow was born in Banbury, England, on June 11, 1957. He received the B.Sc. degree in applied physics and electronics from the University of Durham, Durham, England in 1978.

In 1978 he joined the Optical Communications Group, University of Southampton, Southampton, England, as a Research Student working for the Ph.D. degree on birefringence properties of single-mode fibers. Since October 1981 he has continued his studies as a Junior Research Fellow.

Jens J. Ramskov Hansen (S'76–M'79) was born in Denmark, on July 28, 1952. He received the M.Sc. and Ph.D. degrees in electrical engineering from the Technical University of Denmark, Copenhagen, in 1976 and 1979, respectively.

From 1976 to 1979 he was a Research Fellow at the Technical University of Denmark studying propagation in graded-index fibers. Thereafter, he spent two years as a Hartley Research Fellow at the University of Southampton, Southampton, England, where he was engaged in research in the properties of single-mode fibers. Since September 1981 he has been working on the development of optical fibers for telecommunications at NKT, Copenhagen, Denmark.

Degree of Polarization in Anisotropic Single-Mode Optical Fibers: Theory

JUN-ICHI SAKAI, SUSUMU MACHIDA, AND TATSUYA KIMURA, SENIOR MEMBER, IEEE

Abstract—**The degree of polarization for propagation waves in anisotropic single-mode fibers is formulated in terms of light source spectrum, incident polarization condition, and fiber parameters. The polarization degree deterioration is based on the incident wave split into two eigenpolarization modes inherent in the fiber. Since the two eigenpolarization modes have different group velocities from each other, the degree of polarization is degraded when both of the modes are excited. Polarization degree is preserved when only one of the eigenpolarization modes is excited. The degradation is determined by the mutual correlation function γ, between the two modes, which depends on the light source spectra, fiber polarization dispersion, and fiber length.**

I. Introduction

PRESERVATION of the optical polarized state in fibers is essential to realize coherent optical transmission using the frequency or phase shift keying and heterodyne detection scheme [1]. Fibers which preserve linear polarization have conventionally been studied by many researchers [2], [3]. Recently, a proposal has been made to transmit a circularly polarized light in a twisted single-mode fiber [4]. These works seem to be based on an idea that incident polarized light should be transmitted without polarization conversion.

The state of incident polarization may be changed by a scattering process, external mechanical stresses, ambient changes, and other causes. The apparent degradation in the degree of polarization can be recovered by adjusting retardation at the fiber output [5]. Only intrinsic degradation remains after ideal phase compensation is carried out. It has been shown that proper incident polarization states exist which preserve a high degree of polarization [6], [7]. Polarization mode dispersion has been discussed to explain the polarization degree degradation for linear polarization incidence [8].

The purpose of this paper is to formulate the inherent polarization degree in anisotropic single-mode optical fibers. The degradation mechanism is based on an assumption that any incident polarization state is split into two orthogonal eigenpolarization modes [7], which propagate at different group velocity values. The degree of polarization depends on a mutual correlation function between two eigenpolarization modes.

Section II explains properties of the eigenpolarization modes which play an important role in preserving the degree of polarization. The mathematical definition of the eigenpolarizations, their physical features, their vector expressions, and expansion using them are presented. Section III provides the degree of polarization in terms of light source spectrum and fiber parameters by using a coherency matrix. The degree of polarization is compared with several source spectral profiles. In Section IV, the eigenpolarization modes and the polarization degree are described for a twisted elliptical core fiber, as an example of anisotropic single-mode fibers.

II. Eigenpolarization Modes in Anisotropic Single-Mode Fibers

A. Definition of Eigenpolarization Modes

Polarization evolution in anisotropic single-mode fibers has been treated by means of the modified coupled-mode equations containing coupling coefficients N_{ij} [9]. Eigenpolarization modes correspond to eigenstates with particular shapes and propagation constants, independent of propagation length z, as have been theoretically investigated [10]. A mathematical outline of the eigenpolarization modes will be briefly described.

Electric fields in anisotropic single-mode fibers can be repre-

Manuscript received August 31, 1981; revised November 16, 1981.

The authors are with the Electrical Communication Laboratories, Nippon Telegraph and Telephone Public Corporation, Musashino-shi, Tokyo, Japan.

0018-9480/82/0400-0334$00.75